SIMULATION AND EXPERIMENTAL INVESTIGATION OF POOL BOILING ON A SILICON WAFER WITH ARTIFICIAL NUCLEATION SITES

A. Sanna[1], C. Hutter[2], H.Lin[2], K. Sefiane[2], A.J. Walton[2], E. Pavlovič[3], I. Golobič[4], R.A. Nelson[5], T.G. Karayiannis[1] and D.B.R. Kenning[1]

[1] Brunel University, Uxbridge, UB8 3PH, UK, [2] University of Edinburgh, Edinburgh, EH9 3JL, UK, [3] Hidria Institute Klima, Godovič, Slovenia, [4] University of Ljubljana, Ljubljana, Slovenia, [5] Los Alamos National Laboratory, Los Alamos, NM 87545, USA

Abstract

This paper reports progress on a project to develop a design tool for large arrays of nucleation sites at specified locations to achieve high rates of cooling by pool boiling. The tool will be based on an improved version of a hybrid simulation, in which the 3-D temperature field in the wall is solved numerically, along with simple sub-models for bubble-driven heat transfer that require experimental calibration. Improvements to the computer code and progress with the experiments are reported briefly. The paper focuses on the development of a sub-model for the lateral coalescence of bubbles, which is shown to cause irregularity in the bubble production by a regular array of nucleation sites.

Nomenclature

H	plate thickness	d	distance between sites

Subscripts

AC	after coalescence	BC	before coalescence
b	bubble	C	coalescence
c	contact	d	departure
i,j	site indexes		

1 Introduction

Most applications and studies of nucleate boiling heat transfer have been for metallic surfaces, on which the spatial and size distribution of nucleation sites can only be controlled in a general way during manufacture. Applications of boiling to the cooling of devices micro-fabricated on silicon open the way to the creation of large arrays of closely-spaced nucleation sites of specified micro-geometry. A design tool is required to explore the infinite number of geometrical possibilities. The development of a hybrid model, able to deal with a large number of activation sites, is not straightforward, since phenomena related to bubble growth, detachment and interaction between sites must be described by simple sub-models that are sufficiently flexible to accommodate different phenomena. Comparisons with experimental data and fully 3-D simulations for isolated sites will provide significant help in the development and validation of the model.

The choice of parameter values in the physical sub-models in the hybrid code will depend on information provided by very detailed localized experimental measurements being performed at the University of Edinburgh on boiling of FC-72 and water on arrays of sites with micro-thermometers micro-fabricated on silicon, in a rig described by Hutter et al. (2007), and data from an on-going

investigation at Ljubljana University of pool boiling on very thin metal foils, employing high-speed IR thermography to measure 2-D wall temperature variations, Golobič et al. (2007a).
The code was first developed by Nelson and colleagues at the Los Alamos National Laboratory (LANL) to investigate the influence of wall properties on interactions by conduction between hundreds of sites, Pasamehmetoglu and Nelson (1991). Golobič et al. (1996) at Ljubljana University developed a version of the model in which sites could be placed at any position and the computational grid was refined temporarily in a cylindrical region under every growing bubble. The bubble growth sub-model was a simplified version of the Stephan and Hammer (1994) model for evaporation at a triple contact line, with additional heat transfer in the central contact area. Again, only site interactions transmitted through the wall were included. This paper describes further improvements to the version of the code described by Sanna et al. (2007) and (2008), focusing on the simulation of the coalescence of bubbles of sensibly dissimilar size.

2 Numerical simulation: improvements to code and models

The code has been restructured by Nelson at LANL for parallel computation in order to reduce calculation time. A reorganization of the physical sub-models has increased flexibility and applicability to different conditions. The code solves the 3-D transient conduction equation for the temperature distribution $T(x,y,z;t)$ in a rectangular slab representing the heated wall of thickness H, with the assumptions and conditions specified in Sanna et al. (2007) and (2008). The transient equation is solved by a simple explicit method, with consequent limitations on numerical accuracy and stability. The basic computational Cartesian mesh is temporarily refined in a cylindrical region (composed of a fixed number of concentric rings, six in current simulations, plus a connection area between Cartesian and cylindrical cells) around each active site during bubble growth from nucleation to detachment. Values of the variables and properties are assumed uniform within each cell.
Originally, the mesh radius was refined in a region of fixed radius corresponding to the maximum contact radius, which occurred at detachment and which was specified at each site. Since the code does not permit the overlapping of refined meshes, nucleation of new bubbles had to be prohibited at sites close to a growing bubble, preventing simultaneous growth and coalescence. This constraint has been partially removed, at the cost of increased computing time, by modifying the meshing procedure: the radius of the refined region increases and decreases stepwise so that it is always slightly bigger than the varying contact radius, leading to a variation in cell size during bubble growth. This involves a temporary loss of accuracy in the properties of cells because the code is unable to directly substitute the cylindrical mesh distribution with a new cylindrical distribution without merging the refined area into the original Cartesian cells. To avoid this problem, a new procedure is under study, with a variable number of rings but a constant width of the mesh rings in the refined area.
The current criterion for site activation assumes that a new bubble commences when the local wall superheat exceeds a fixed value specified for each potential nucleation site, provided the previous condition on distance from a growing bubble is satisfied. An improved criterion for activation, including the effect of the temperature gradient at the potential nucleation site, is being developed.
In the original version of the code the bubble was assumed to grow as a truncated sphere with a constant apparent contact angle ϕ. Heat for evaporation was supplied only through the base of the bubble based on the Stephan and Hammer (1994) contact line concept, as described in Golobič et al. (2004). Heat transfer from the bulk liquid through the dome was neglected. The latest version of the code includes a sub-model for heat transfer to the dome, as discussed in Sanna et al. (2007) and (2008). Heat transfer through the base of the bubble is driven by specifying values for the heat transfer coefficient in each ring of the refined mesh. In order to approximate the Stephan and Hammer (1994) model with a pure contact line model, a very high heat transfer coefficient is specified only in the ring containing the contact line with an adiabatic dry spot for the contact area. Its value is based on experimental observations of bubble growth. The product of heat flux and area

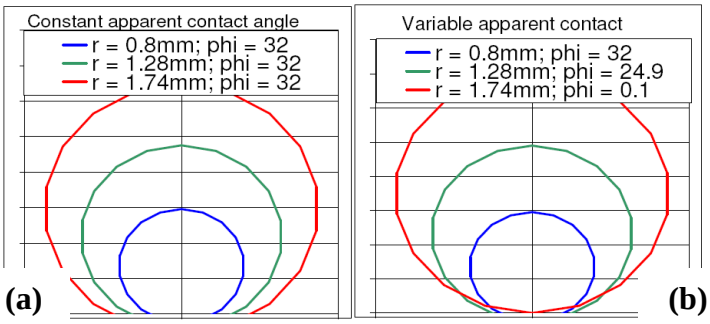

Figure 1a, b: *Apparent contact angle models (a) constant, (b) variable*

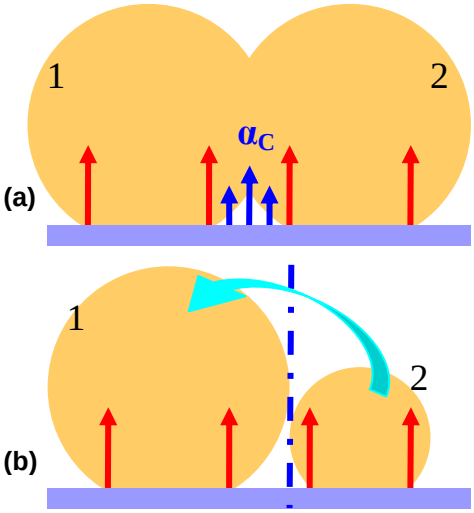

Figure 2a, b: *Coalescence models*

is consistent with the values of heat flow through the much smaller area in the contact zone model. In the examples in this paper the heat transfer coefficient in the inner rings is set to zero. The initial assumption of constant apparent contact angle, which resulted in sudden detachment when the contact area was a maximum, has been replaced by a variable angle, constant during the first stage of the bubble growth and linearly decreasing with the inverse of the volume afterwards, Figure 1(a, b). Bubble detachment occurs when the bubble reaches its maximum volume at a specified bubble departure radius for each site, now coincident with zero apparent contact angle and contact area. It also occurs if the refined mesh areas of two bubbles come into contact: the smaller bubble is assumed to detach instantaneously and the larger bubble continues to grow without detaching. The bubble departure radius is specified on the basis of experimental evidence, highlighting the importance of experiments in tuning the code, as well as subsequent validation.

The conditions for detachment have now been extended by a very simple model to account for coalescence. Two situations are considered, both of which were observed in Golobič et al. (2007b):

(a) If the bubbles have similar size, they are assumed to continue growing as two independent isolated bubbles. A dedicated heat transfer coefficient, α_C, not contributing to the growth of the bubble, will be imposed in the region between them, as shown in Figure 2a. In reality the bubble assumes the shape of a horizontal elongated bubble. The dedicated heat transfer coefficient has not yet been implemented. As a simple temporary measure, the bubbles are allowed to continue growing with overlapping domes but separate contact areas to their specified departure radii or until their refined meshes (which are slightly larger than the contact radii) touch, whereupon the smaller bubble detaches.

(b) If the sizes are sensibly dissimilar, so that the bubble radii ratio is larger than 2, the smaller bubble is assumed to be immediately absorbed by the larger bubble, which undergoes a sudden increase in volume, as shown in Figure 2b. Coalescence occurs when the projections of the domes of the bubbles come into contact. The bubble departure radius, $r_{bd,i}$, of the larger bubble after coalescence is then temporarily increased by a factor dependent on the ratio of the volume of smaller bubble at the time of coalescence, V_j, and the maximum volume of the larger one, $V_{d,i}$, as shown in equation (1).

$$r_{bd,i}(t_{AC}) = 1.015 \cdot \left[1 + \frac{V_j(t_{BC})}{V_{d,i}}\right]^{1/3} \cdot r_{bd,i}(t_{BC}) \qquad (1)$$

This device avoids immediate departure of the larger bubble if coalescence occurs close to its maximum size. A further improvement, not yet introduced, will impose a rapid detachment process with reduction of contact area for the smaller bubble prior to absorption by the larger bubble.

The model at present considers coalescence only between pairs of bubbles in contact with the surface. In circumstances that might lead to simultaneous coalescence of several bubbles, the code forces events to occur sequentially by checking the candidates for coalescence in a regular order

and calculating the consequences before moving to the next candidate. This is consistent with the limited evidence from experiments, e.g. Bonjour et al. (2000), and 3-D simulation (Mukherjee and Dhir, 2004) that multiple coalescences tend to occur sequentially. For reasons of numerical stability, the maximum number of coalescence events for the same bubble is at present limited to six.
The model does not consider coalescence between an attached bubble and a detached bubble. Vertical coalescence between bubbles produced from the same site at very small waiting times was found by Shoji et al. (2005) to have only a small influence on heat transfer and the activity of other sites, so its omission may not be serious. Declining coalescence with a detached bubble from another site was found to have a much stronger influence, although this was not detected by Golobič et al. (2007b). The modelling of declining coalescence will be reviewed when further evidence is available from the experiments at the University of Edinburgh.

3 Preliminary numerical results

Simulations for constant bubble departure radius have been run by varying the spacing *d* between the sites, to study its effects on thermal interaction between sites and coalescence, as studied experimentally by Shoji et al. (2005). This is a preliminary study to support the design of silicon wafers with micro-machined cavities for use in the experiments with FC-72, as in Hutter et al. (2007) and in Section 4 of this paper.

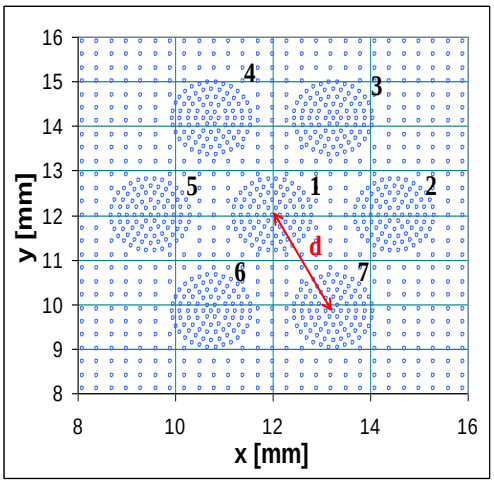

Figure 3: *Mesh distribution*

In order to reduce computational time, the geometry used in the simulations is a square silicon plate, 24 x 24 mm, 0.38 mm thick, divided into 6 vertical layers for computation. The plate has seven potential activation sites located at its centre, arranged in triangular symmetry. The site activation temperature is 115.5 °C, and the bubble departure radius is 1.75 mm, based on Shoji et al. (2005), with an initial apparent contact angle of 32°. A uniform volumetric heat source corresponds to an input heat flux of 50 kW/m^2. The bottom of the plate is adiabatic and its edges are kept at constant temperature of 125.01 °C. This value, approximately corresponding to the steady state temperature that would be obtained if the enhanced natural convection coefficient was supposed, and used also as the initial condition for the top surface, has been employed to reduce the total dimensions of the plate, in order to use a finer distribution of unrefined Cartesian meshes. The mesh distribution on the central area of the plate (8x8 mm) when all the sites, with a spacing of *d=2.5 mm*, have been activated is shown in Figure 3, each dot corresponding to the centre of a cell. Interference between the refined meshes cannot occur for these conditions.
The bubble radius ($r_{b,i}$), the contact area radius ($r_{c,i}$) and the nucleation site temperature (T_i) at the central site 1 and at sites 2 and 5 are compared in Figure 4 for *d=4.0 mm* (thermal interaction only) and in Figure 5 for *d=2.5 mm* (thermal interaction plus coalescence, models a + b). In the absence of coalescence, sites 1, 2 and 5 produce bubbles regularly, Figure 4, with no waiting time. The

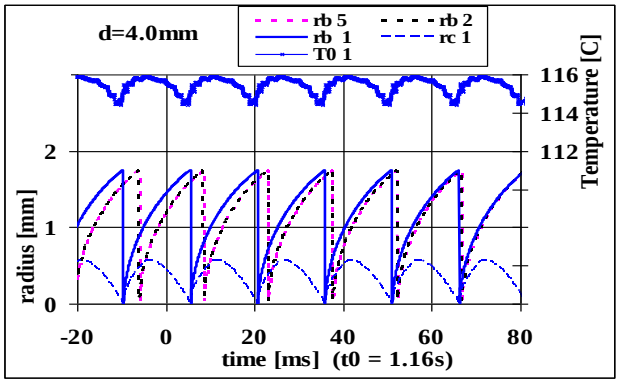

Figure 4: *Radius and temperature distributions for d=4.0mm*

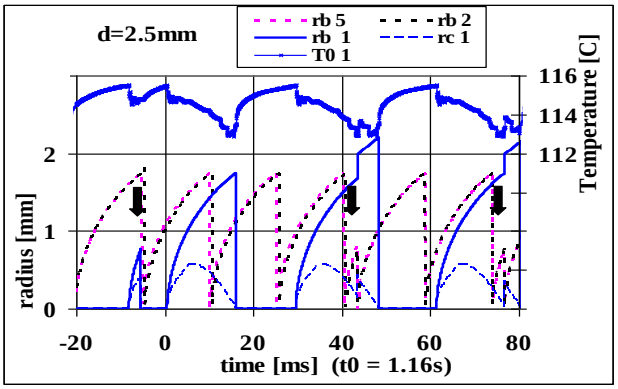

Figure 5: *Radius and temperature distributions for d=2.5mm*

frequency is slightly lower at site 1 because it receives heat by lateral conduction from a smaller area of the plate that is also cooled down by the surrounding sites. Consequently, bubble production at site 1 and sites 2 and 5 is out of phase. Sites 2 and 5 are in identical positions but they develop very slight differences, presumably due to procedures in the numerical code: solution of the conduction equation, mesh refinement, numerical rounding errors. The code will be verified more thoroughly after implementation of the new procedure for mesh refinement. After activation at 115.5 ^{o}C, the temperature at site 1 (Figure 4) increases to 116 °C, hovering before the final stage of detachment, when the high heat transfer coefficient at the slowly contracting contact line causes a large reduction in temperature. Immediately after detachment, the site temperature rapidly increases to the activation temperature at a rate that determines no waiting time, corresponding to the continuous bubbling with vertical coalescence observed by Shoji et al. (2005). The changes in temperature at the nucleation sites depend strongly on the use of the pure contact line model and on the value of the heat transfer coefficient at the contact line, highlighting the necessity of refining the mesh. Increase of the heat transfer coefficient leads to higher heat removal in the central area and a significant waiting time. Horizontal coalescence is impossible according to the current model for $d=4$ *mm* and $r_{bd}=1.75$ *mm*, but Shoji et al. (2005) found that coalescence became negligible only for $d > 3 \cdot r_{bd} = 5.25$ *mm*, presumably because of fluctuations in departure radius. In principle, random variability in the specified departure radius could be incorporated in the model.

When the spacing is reduced to $d = 2.5$ *mm*, site 1 is partially cooled by surrounding sites leading to a lower temperature and consequent significant waiting time. Simultaneous type (a) coalescence of bubbles at all the sites would be expected if their thermal conditions were identical. The phase difference between growth at site 1 and the other sites opens the way to type (b) coalescence between bubbles of dissimilar size with radii ratio > 2. As for $d = 4$ *mm*, there are slight differences between the identical sites 2 and 5 that may arise from the numerical procedures, to which is now added the effect of the sequence in which near-simultaneous coalescences are executed. In Figure 5, it is seen that events at the two sites are closely synchronized, except for a short time after a coalescence: differences in average bubble frequency are less than 1.33% over the simulating time of 2.0 s.

Three close type (b) events (a very rare occurrence) are marked in Figure 5 by ⬇. At -5.4 ms, a small bubble at site 1 is absorbed by a large bubble at site 2. The bubble at 1 is removed, creating an additional rise and fall in the temperature at site 1, Figure 5; the absorbing bubble has a slight instantaneous increase in radius and a small increase in its detachment radius calculated by equation (1). At +43.6 and +76.7 ms, a large bubble at 1 absorbs in quick succession small bubbles at all the surrounding sites, including 2 and 5, causing an increase in its radius and departure radius; the temporary expansion of the contact radius moves the region of intense cooling outwards, causing a rise and fall in the temperature at site 1, Figure 5. Table 1 summarizes the data for dissimilar coalescence events involving site 1 over a simulated period between 0.6 s and 2.0 s, showing that site 1 is more likely to absorb a bubble than be absorbed. The second type of event exhibits significant variability between sites. In addition, there are type (a) coalescences between bubbles of similar size at site 1 and the surrounding sites that, according to the current model, do not cause thermal disturbances.

The cooling effect of the group of sites with d = 2.5 mm is illustrated in Figure 6. The temperature continuously decreases from its boundary value of 125.01 °C and particularly, the temperature of the wall surrounding site 1, which is influenced by all the sites, does not exceed 116 ^{o}C, causing the lower rate of bubble production at that site and a large waiting time. The expanded plot of the wall surface temperature on a line passing through sites 5 - 1 - 2 in Figure 7 shows a slight asymmetry between sites 2 and 5 in the relative timing and sizes of their bubbles, causing larger asymmetries in the instantaneous distributions of heat flux and heat transfer coefficient in Figures 8, 9.

At +8 ms, the domes of the smallest bubble at site 1 and the slightly bigger bubbles at 5 (left) and 2 (right) overlap as a consequence of an earlier type (a) sequential coalescence. At +43.36 ms, the very small bubbles of slightly different size at 5 and 2 are about to be absorbed by the large bubble at 1 in the sequential type (b) coalescence at + 43.6 ms. When the code has been thoroughly verified, it will be used to explore whether small fluctuations in local conditions in the simulation,

which might well occur in a physical situation, lead to growing irregularities because of the strongly nonlinear dynamics of the activation of nucleation sites.

Table 1: *Summary of coalescence*

	i=2	i=3	i=4	i=5	i=6	i=7	average
$r_{b,1} > r_{b,i}$ → bubble at site 1 absorbs bubble at site i							
f_i [Hz]	10.71	10.71	10.00	10.00	10.00	10.00	10.24
$r_{b,1} / r_{b,i}$ average	2.43	2.43	2.34	2.25	2.37	2.50	2.39
$r_{b,i} > r_{b,1}$ → bubble at site i absorbs bubble at site 1							
f_i [Hz]	6.43	0.71	0.71	0.71	0.00	0.71	1.54
$r_{b,i} / r_{b,1}$ average	0.45	0.49	0.45	0.50	0.00	0.46	0.39

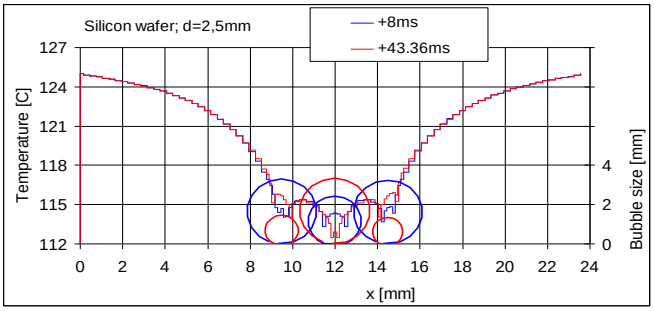

Figure 6: *Temperature distribution for d=2.5mm*

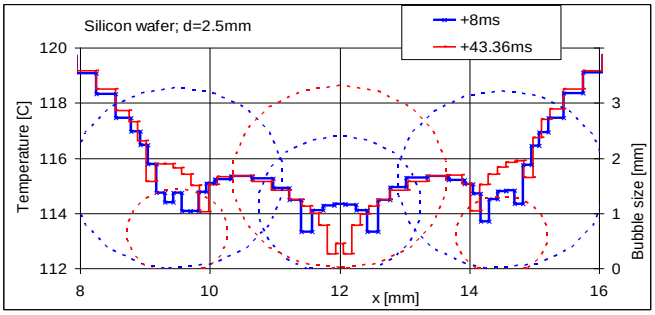

Figure 7: *Local temperature distribution*

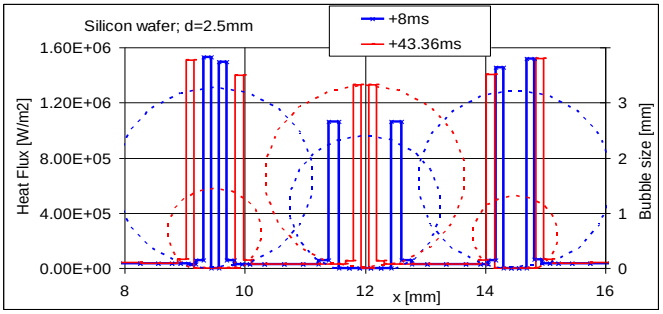

Figure 8: *Heat flux*

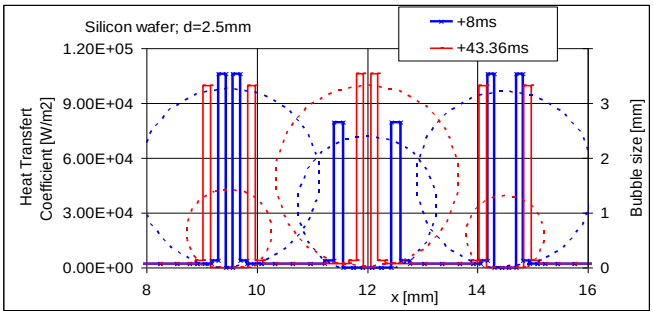

Figure 9: *Heat transfer coefficient*

4 Preliminary experimental studies on silicon

The simulation code depends on experimental input for the values of parameters driving bubble growth and detachment. It then predicts local wall temperature and heat flux, leading to predictions of the activation of sites, which require verification by experimental measurements. The development of the code depends on a continuous interaction with an experimental programme.

Some experimental data for pool boiling of water on very thin metal foils at Ljubjana University have indicated that heat transfer to a bubble may be distributed over a larger part of its contact area than is assumed in the contact line model currently used in the code, Golobič et al. (2007a,b). It is not known whether this observation also applies to boiling on silicon wafers. Simulations with an earlier version of the code, Pavlovič (2005), showed that the distribution of heat transfer influenced the temperature changes at the nucleation site. Preliminary simulations with the current version of the code, Sanna et al. (2007) and (2008), using the same contact line model for water boiling on a 25 μm titanium foil and on a 0.4 mm silicon wafer, showed that bubble growth was more rapid with much shorter waiting times on the silicon wafer.

It is necessary to perform boiling experiments on silicon wafers with artificial sites to establish appropriate modelling assumptions and inputs for the inception, growth and detachment of individual bubbles and thermo-fluid interactions between sites, including coalescence. Finally, the

pattern of interactions in large arrays of artificial sites will be measured by integrated micro-resistance thermometers embedded in the silicon under about 100 nucleation sites.
A pool boiling rig described by Hutter et al. (2007) was recently built at the University of Edinburgh. In order to reduce the practical problems of electrically insulating the connections to the micro-sensors, the preliminary experiments are being performed with the dielectric fluid FC-72.
The commissioning tests were performed with a silicon wafer with 45 cylindrical sites, diameter 2 μm and estimated depth 22 μm, in a square array of pitch 10 mm without micro-sensors. Heating was provided by a separate thin electrical resistance heater attached to the rear of the wafer. The growth and detachment of individual bubbles was recorded by high-speed video camera and these measurements provided preliminary estimates for the parameters used in the simulations in this paper. The tests also confirmed the anticipated difficulty of visually recording the activity of all the sites in a large array, because of obstruction by bubbles from other sites. Some bubbles originated from sites other than those in the artificial array, indicating the presence of small surface defects and the need for rigorous cleaning.
The second test section has five cavities of diameter 2, 5, 10, 20 and 50 μm, depths 62.5, 74.7, 82.8, 82.8, 86.1 μm respectively, each positioned above a micro-sensor, Figure 10. Heat is provided by an integral thin-film resistance heater (95% Al, 4% Cu and 1% Si) on the rear of the 0.38 mm thick silicon wafer, inside the red rectangle in Figure 11. The nickel micro-thermometers are calibrated individually and have a near-linear increase of electrical resistance with temperature. The cavities were all activated at a heat input flux of 1.2 kW/m^2 and cavities 1,3,4,5 remained active after a reduction to 0.19 kW/m^2, Figure 12. The fluctuating temperature measured under cavity 3 in fully-developed boiling at 16.6 kW/m^2, shown in Figure 13, may have been influenced by bubbles produced at other sites that have still to be controlled.

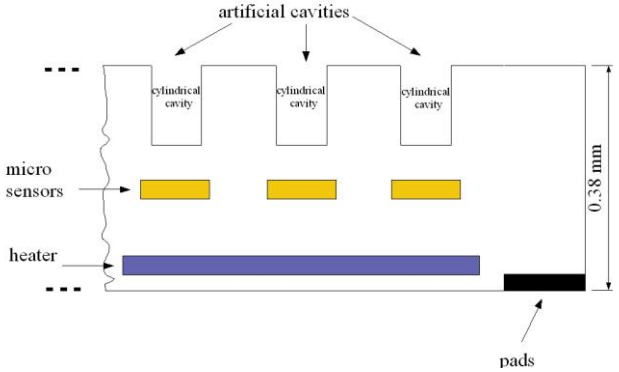

Figure 10: *Schematic arrangement of sensors*

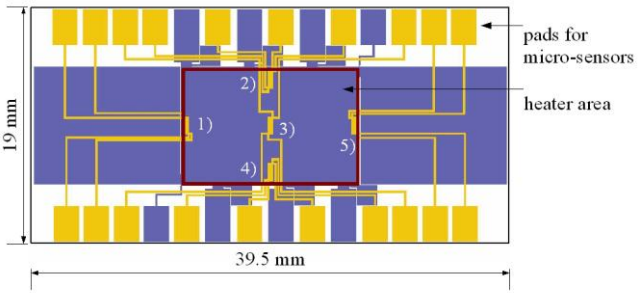

Figure 11: *Test section layout*

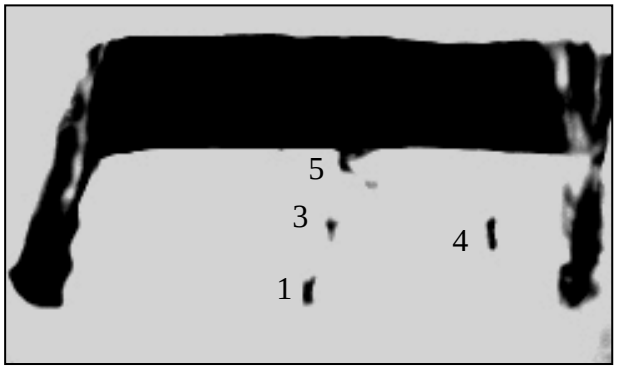

Figure 12: *Nucleation sites 1, 3, 4, and 5 active at 0.19 kW/m^2*

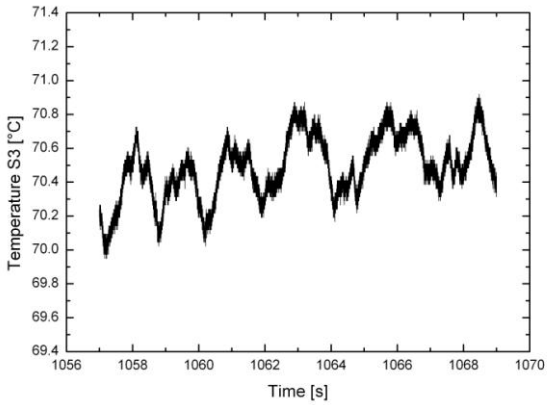

Figure 13: *Fluctuating temperature under cavity 3 at 16.6 kW/m^2*

5 Conclusions

Progress has been made towards the development of a design tool for array of nucleation sites for the cooling of silicon chips by pool boiling. The physical sub-models and numerical procedures in a simulation code originally developed over 1991-1996 have been improved. A model for bubble coalescence suggests that coalescence may promote irregularities in the nucleation of bubbles at a regular array of nucleation sites. The model requires further development. Micro-instrumentation to measure local temperatures and hence detect nucleation at individual sites in a large array has been fabricated and calibrated successfully.

Acknowledgement

This project was supported by the Engineering and Physical Sciences Research Council of the UK (Grant EP/C532805/1 and E P/C532813/1).

References

Bonjour, J., Clausse, M., Lallemand, M., 2000, Experimental study of the coalescence phenomenon during nucleate pool boiling, Experimental Thermal and Fluid Science Vol. 20, pp. 180-187.

Golobič, I., Pavlovič, E., and Strgar, S., 1996, Computer model for nucleation site interactions on a thin plate, Proc. Eurotherm Seminar No. 48, Pool Boiling 2, Paderborn, pp. 33-42.

Golobič, I., Petkovsek, J., Baselj, M., Papez, A., Kenning, D.B.R., 2007a, Experimental determination of transient wall temperature distributions close to growing vapor bubbles, Heat Mass Transfer On-line DOI 10.1007/S00231-007-0295-y.

Golobič, I., Petkovsek, J., Kenning, D.B.R., 2007b, Bubble growth and horizontal coalescence in saturated pool boiling on a thin foil, investigated by high-speed IR thermography, submitted to Int. J. Heat Mass Transfer.

Hutter, C., Sefiane, K., Walton, A. J., Karayiannis, T. G., Kenning, D. B. R., 2007, Pool boiling investigations on silicon with artificial cavities, immersed in FC-72, UK National Heat Transfer Conference, September 2007.

Mukherjee, A., Dhir, V.K., 2004, Study of lateral merger of vapor bubbles during nucleate pool boiling, J. Heat Transfer Vol. 126, pp. 1023-1039.

Pasamehmetoglu, K.O. and Nelson, R.A., 1991, Cavity-to-cavity interaction in nucleate boiling: the effect of heat conduction within the heater, AIChE Symposium Series (27th Nat. Heat Transfer Conf., Minneapolis), Vol. 87, pp. 342-351.

Pavlovič, E., 2005, Doctoral Thesis, University of Ljubljana, Faculty of Mechanical Engineering.

Sanna, A., Kenning, D.B.R., Pavlovič, E., Golobič, I., Sefiane, K., Karayiannis, T.G. and Nelson, R.A., 2007, Critical analysis and improvement of a mechanistic multi-site model for pool nucleate boiling, UK National Heat Transfer Conference, September 2007.

Sanna, A., Karayiannis, T.G., Kenning, D.B.R., Hutter, C., Sefiane, K., Walton, A. J., Golobič, I., Pavlovič, E., and Nelson, R.A., 2008, Steps towards the development of an experimentally verified simulation of pool nucleate boiling on a silicon wafer with artificial sites, Submitted to Applied Thermal Engineering.

Shoji, M., Zhang,L., and Chatpun, S., Nucleation site interaction in pool nucleate boiling – Serial experiments using artificial boiling surfaces -, 6th World conference on experimental heat transfer, fluid mechanics, and thermodynamics, April 2005

Stephan, P. and Hammer, J.,1994, A New Model for Nucleate Boiling Heat Transfer, Wärme- und Stoffübertragung Vol. 30, pp. 119-125.